

AERODYNAMIC ANALYSIS OF THE USE OF MULTI-WINGLETS IN LIGHT AIRCRAFTS

Cosin, R., renatocosin@uol.com.br

Catalano, F. M., catalano@sc.usp.br

Aerodynamic Laboratory – São Carlos Engineering School – University of São Paulo – São Paulo – Brazil

Abstract. *The major objective of this work is to analyse the aerodynamic characteristics of multi-winglets applied to light aircrafts. This wing tip device has demonstrated a potential of improving the aerodynamic efficiency of aircrafts by the reduction on the induced drag. The data discussed were results of experimental investigations for a wing-body half model at $Re=4 \times 10^5$ with six different multi-winglet configurations plus the base line. It was achieved up to 7.3% of increase on maximum aerodynamic efficiency and even greater values for others medium to high lift coefficient regimes. A performance analysis was also conducted revealing a potential increase of 12% on maximum climb ratio. The pressure distribution over the wing was measured, leading to conclusions about the global and local effects of the device on the wing loading. A wake study from a seven hole pitot probe mapping downstream the wing and structural loading investigation complete this research.*

Keywords: multi-winglets, induced drag, tip sails, aerodynamic efficiency

1. INTRODUCTION

The now days major requirements of an aircraft lead to the necessity of more efficiency. On this contest, the drag reduction plays a central role for the success of an airplane either on accomplishing its mission or on commercial aspects. In this scenario, the scope of this study is to investigate the potential use of multi-winglets to enhance the efficiency and performance of aircraft by reducing the induced drag.

Generating lift on a finite wing implies on the presence of the wing tip vortex as an unavoidable collateral effect that reduces the lift of the wing and generate a significant amount of drag, particularly known as induced drag.

It has been proven that modifications on the wing tip or the use of wing tip devices can reduce in expressive amounts the induced drag, improving the wing efficiency. Extensive investigations have been conducted with the objective of studying these devices, as well proposing new design and approaches.

Modifications of the wing tip can either move the vortices away in relation to the aircraft longitudinal axis or reduce their intensity (Kravchenko,1996). Some of these devices such as winglets, (Whitcomb,1976), tip-sails (Spillman, 1978), (Spillman and McVitie, 1984), (Spillman,1987) and multi-winglets ,(Smith and Komerath,2001), take advantage of the spiraling airflow in this region to create an additional traction, and reducing the induced drag.

Whitcomb [3] showed that winglets could increase wing efficiency by 9% and reduce induced drag by 20%. Other devices break up the vortices into several parts, each with less intensity facilitating dispersion, which is important, for instance, for the decrease of the interval time between takeoff and landings in large airports (La Roche and Palfy,1996). (Kravchenko,1996). tested and compared different shapes of wing tips: winglets and tip-sails. The winglets presented higher aerodynamics benefits up to Mach 1.0, however they also presented structural problems for the aircraft due to the increase in bending moment at the wing root.

Tip-sails, at low lift coefficient, provided the same benefits; nevertheless, the bending moment at the wing root was less. Research with agricultural aircraft has also been made comparing wing-tip devices, (Coimbra, R and Catalano, 1999). For this category of aircraft, besides both aerodynamic and structural advantages, the influence of the vortices created during the mission of the aircraft is an added parameter in the analysis.

Winglets have been used to improve sailplane performance. (Smith and Komerath,2001) mentions the development work on winglets for sailplanes tested in a wind tunnel with scale models.

2. EXPERIMENTAL CONFIGURATION

The tests were carried out in the LAE 2 closed circuit low speed wind tunnel, with a turbulence level of 0.25% at 30m/s. The test section has 1.7 m of width, 1.3 m of height and 3.6m of length,(Catalano,2001). The Reynolds number used was $Re=4 \times 10^5$ except for the wake measures which was conducted with $Re=4 \times 10^5$.

2.1. General model characteristics

For the present research, was designed and built a half model based on a high wing single engine trainer aircraft under development on Engineering School of São Carlos. The model consists on a wing-body configuration with 1:6 scale. The wing has no taper nor sweep. The dihedral is 1.5° and the washout is 1.25° . It was used the NACA 23015 airfoil in the entire span and the full span aspect ratio is 8.

The fuselage was designed to accommodate in fully closed compartments all the pressure scanners modules as well its installation accessories. Its wing support allows adjusting the dihedral and incidence of the wing. The model wing has a chord of 216.5 mm and was built with a very smooth surface to avoid unintentional forced transition. On the upper and lower surface there are a total of 248 measure points in 8 wing sections, with higher concentration of points near the leading edge and the wing tip. The model also includes a 30 mm stand-off to minimize the effects of the tunnel boundary layer.



Figure 1: Model prepared for tests, left, and multi-winglets in configuration 1, right

2.2. Variable configurations multi-winglets

The wing tip device is a variable configuration multi-winglets with three tip sails. Those are attached to a movable mechanism that allows the adjustment of the cant angle and incidence of the winglets. The lock is made by four screws, what make possible to vary the cant angle and incidence for each sail independently. All the pieces of the device were executed by fast prototyping process called SLS “selective laser sinterization” using polyamide.

For this study were selected six configurations to be compared with the baseline. The cant angles combinations are listed on “Tab 1” and are base on (Cerón Muñoz and Catalano, 2004) best results. Due to the objective of studding the lift dependent induced drag, wasn’t used any transition strip during most of the tests, although the forced transition case was compared with the untripped wing case what revealed lower lift coefficient levels, not realistic with the expected full scale Reynolds number condition. No global stall characteristics changes due to the forced transition were detected.

The three sail are non swept and have taper of 0.45 and aspect ratios of 2.7, 3.1 and 3.5 respectively. The profiles, twist distribution and other geometric parameters were defined from CFD simulations of the flow around the baseline wing tip considering the base principles of winglets.

Table 1. Selected cant angle configurations

Configuration	Cant Angle			Configuration	Cant Angle		
	Winglet 1	Winglet 2	Winglet 3		Winglet 1	Winglet 2	Winglet 3
1	-30	0	30	4	60	30	0
2	45	15	-15	5	45	30	15
3	-15	-30	-45	6	30	15	0

2.3. Instruments and measures

For the investigation off the several aerodynamics characteristics and effects of the multi-winglets were selected a wide range of measures types to be executed during the wind tunnel testing. The primary data is the 2 axis balance measures that give the aerodynamic forces on the model, which allow calculating many of the most important coefficients.

It was also measured the pressure distribution on the wing surface with three pressure scanners linked with the orifices on the wing. These data is used to determine either the global and local effects of the multi-winglets on the aerodynamic loading of the wing. The pressure scanners are from Scanivalve corp.[®] and have a scale range of ± 2.5 psi and an accuracy of $\pm 15\%$ FS with a sample rate of 2kHz. Additionally, it was installed a stain gage on the wing spar, which supports the entire load. This device can measure the bending moment on the wing root, what make possible to verify the influence of the device on structural loading .The measures of the velocity field downstream the wing uses a seven holes pitot probe with eight piezoresistive pressure transducers, seven for the probe and one for the reference.

4. RESULTS AND DISCUSSION

3.1. Wind tunnel corrections

The correction for the effects of wind tunnel walls and stand-off were done using CFD simulations of baseline configuration and comparison of these results with respective experimental data. The solver used was the ANSYS™ CFX11®, with Shear Stress Transport turbulence model and Gama-Theta transition model. The mesh generation was done with ANSYS™ Icem CFD11®.

The unstructured mesh was generated based on the real geometry of the model, which was scanned with a high precision tridimensional measuring arm. The geometry was built in Dassault Systèmes™ CATIA V5® CAD software from the model surface scan data. A mesh convergence and numeric results validation study was made using the wind tunnel boundary conditions in the simulations. Once validated, the numeric model was solved for the confined flow conditions as well for the free flow. These final data were used to determine the correction coefficients in functions established from analytical knowledge.

3.2. Aerodynamic characteristics

3.2.1. Lift and drag influence

The main influences of the use of multi-winglets are in the lift and drag of the wing. The data obtained from the measured aerodynamic forces revealed a significant increase in the lift curve slope in comparison with the basic wing leading to greater lift coefficient to most of angles of attack as seen on “Fig 2”. It can be explained mainly by the increase on the wing loading near the tip, noticed on “Fig 8” and “Fig 9” in addition to the lift of the each winglet itself, even with their small area. The lift curves slope was augmented from 4.8 up to 5.3, an increase of 11%.

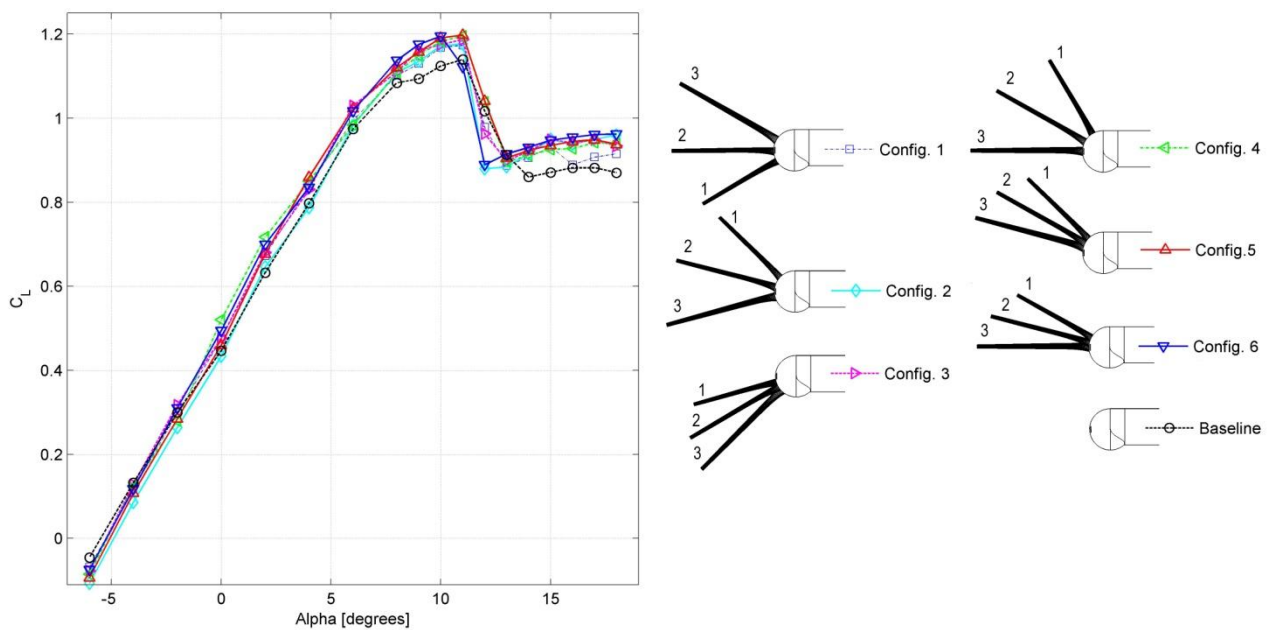


Figure 2. Lift coefficient curve with illustrated legend for the studied configurations

An improvement on the maximum lift coefficient is also observed in the six studied configurations as seen on “Fig 2”. The angle of attack for the stall is near the same for all the configurations and the basic wing. The maximum lift coefficient increased from 1.14 up to 1.20.

The effects of the multi-winglets on the drag at most of angles of attack are of small magnitude. It can be seen that for small angles of attack, up to 2°, the device produce a little more drag than the basic wing. For higher angles as seen on “Fig 3”, the reductions of the induced drag become more expressive and the total drag is slightly reduced until the stall, were this analysis is not of interest. These characteristics are consequence of the combination of the additional zero lift drag caused by the sails in addition to the reduction of the induced drag, that is intended to prevail for most conditions.

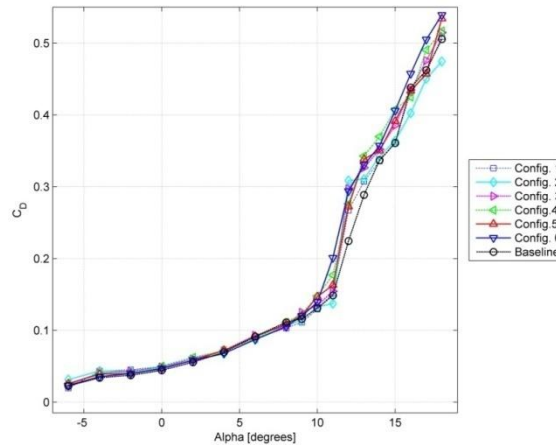


Figure 3. Drag coefficient curve

“Figure 4”, which combine the lift and drag data, shows that the origin of the increases in the efficiency are a combination of greater lift with a slightly lower drag. This effect are due to the reduction of the effect of the wing tip vortex over the wing, what reduces the losses of lift as consequence of a weak and spread tip vortex system, as well significantly decrease the induced drag, as noticed in “Fig 5” by the lower slope of the induced drag curve from wings with multi-winglets.

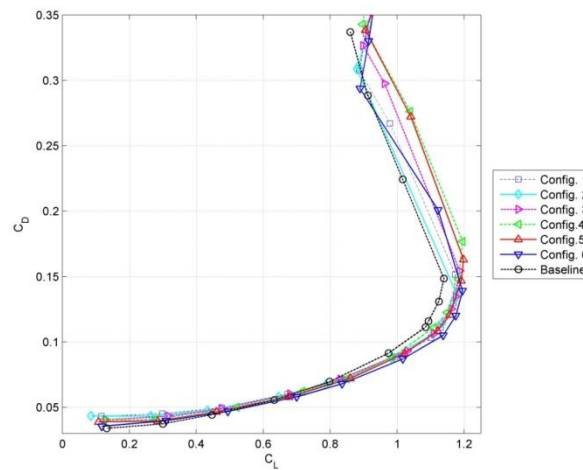


Figure 4. Drag polars

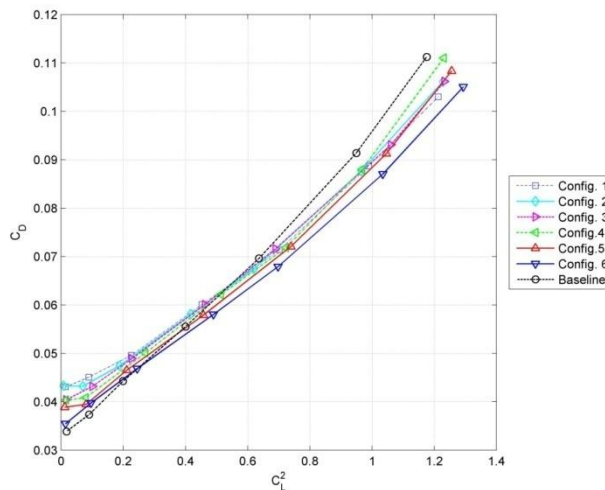


Figure 5. Induced drag curve

The reductions on the lift dependent drag can also be seen by the significant increase in the Oswald efficiency factor, as shown in “Tab 2”. It was observed an undesirable significant increase on the zero lift drag, what makes the device to become more efficient only for lift coefficients greater than 0.4 to 0.5, depending on configuration, despite the clear reduction on induced drag. This negative effect is overestimated on the wind tunnel tests due to the low Reynolds number related to the sails chord, which maximum value is $Re=0.7 \times 10^4$.

Table 2. Aerodynamic parameter from experimental data to various configurations

Configuration	$C_{L\alpha}$	e	C_{D0}	$L/D_{m\acute{a}x}$
1	5.081	0.855	0.040	11.742
2	5.131	0.846	0.040	11.678
3	5.117	0.787	0.038	11.595
4	5.078	0.796	0.037	11.831
5	5.335	0.781	0.036	11.930
6	5.141	0.801	0.035	12.295
Basic wing	4.822	0.648	0.032	11.456

3.2.2. Pressure data

Analyzing the pressure distributions from the wind tunnel tests, it’s possible to observe that the changes in the aerodynamic loading on the wing are of small magnitude. However, as seen on “Fig 6” to “Fig 9”, is noticed a little increase in the loading from the tip by about 20% of the span, as expected by the increases on the lift. A high pressure region on the upper surface of the wing near the tip and the trailing edge present due to the tip vorticity was perceptibly reduced with the use of the winglets, as seen on “Fig 6” to “Fig 9”. This effect is another source of lift gain. Both this phenomena is also a clear indication of the reduction of the effect due to the wing tip vortex on the wing loading, what also reduces significantly the induced drag.

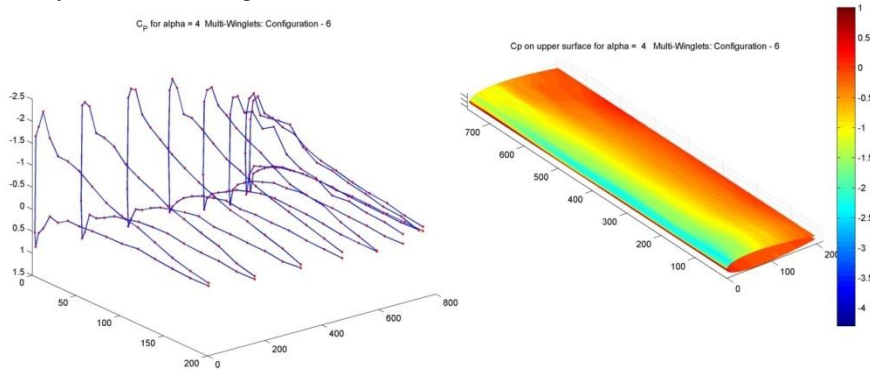


Figure 6. Pressure coefficient distribution over the wing for the sixth configuration with $\alpha = 4^\circ$

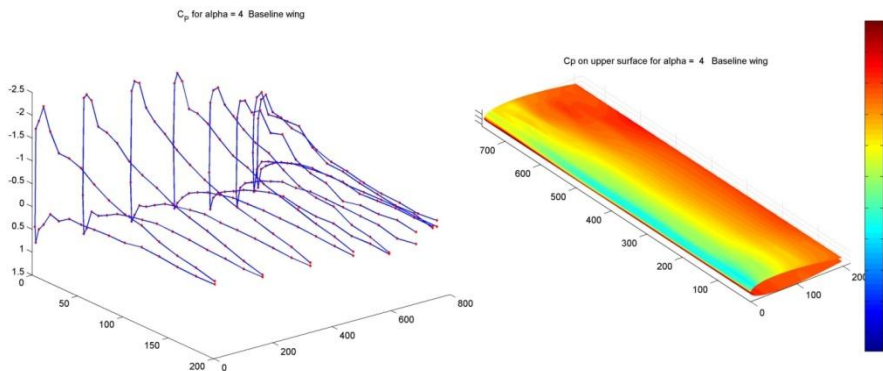


Figure 7. Pressure coefficient distribution over the wing for the baseline configuration with $\alpha = 4^\circ$

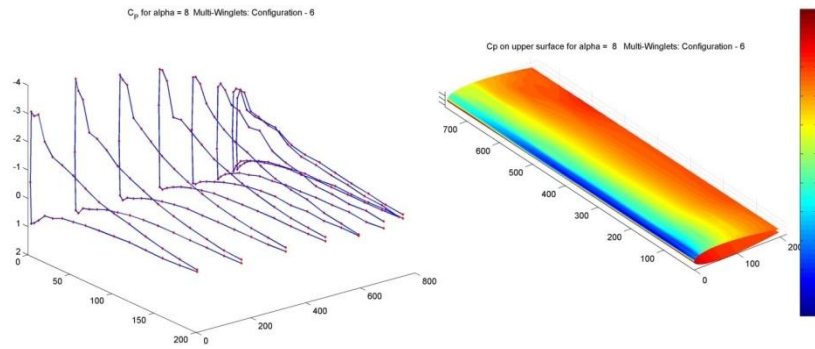


Figure 8. Pressure coefficient distribution over the wing for the sixth configuration with $\alpha = 8^\circ$

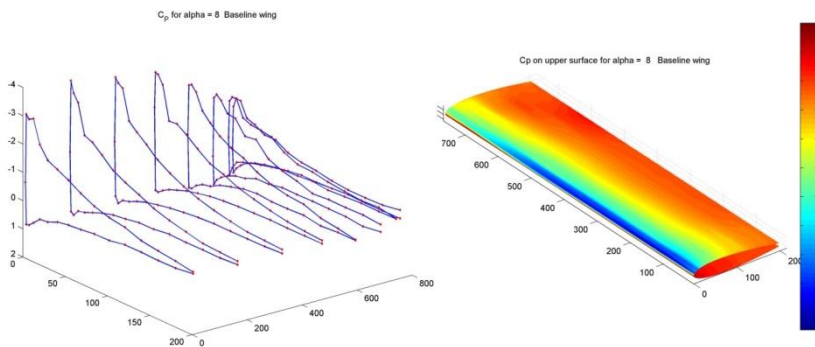


Figure 9. Pressure coefficient distribution over the wing for the baseline configuration with $\alpha = 8^\circ$

From the pressure data were also observed that the multi-winglets don't change the stall main characteristics of the wing. In spite of small variations on the stall angle of attack, the separation region is almost the same for the basic wing and other investigated configurations, as observed on "Fig 10" and "Fig 11".

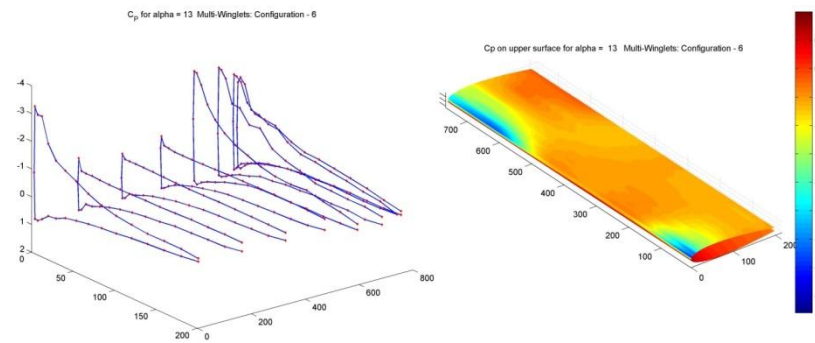


Figure 10. Pressure coefficient distribution over the stalled wing for the sixth configuration with $\alpha = 13^\circ$

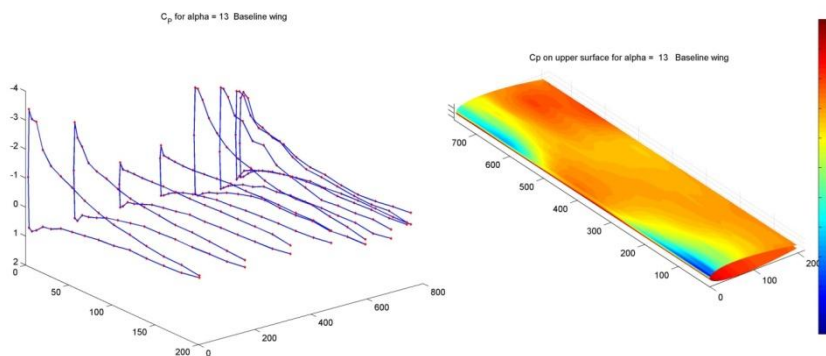


Figure 11. Pressure coefficient distribution over the stalled wing for the baseline configuration with $\alpha = 13^\circ$

3.2.3. Wake analysis

The tridimensional velocity components mapping downstream the wing was realized in a fixed α of 4° , for the basic wing and three of the studied multi-winglets configurations. The velocity contour shows a very expressive change on the tip vortex relative to the baseline, as shown on “Fig 12” and “Fig 13”. As expected the winglets reduced the intensity of the main tip vortex and break up the vortices to the sails tip. These sail tip vortex presented different aspects in the various configurations, as seen on “Fig 12” and “Fig 13”.

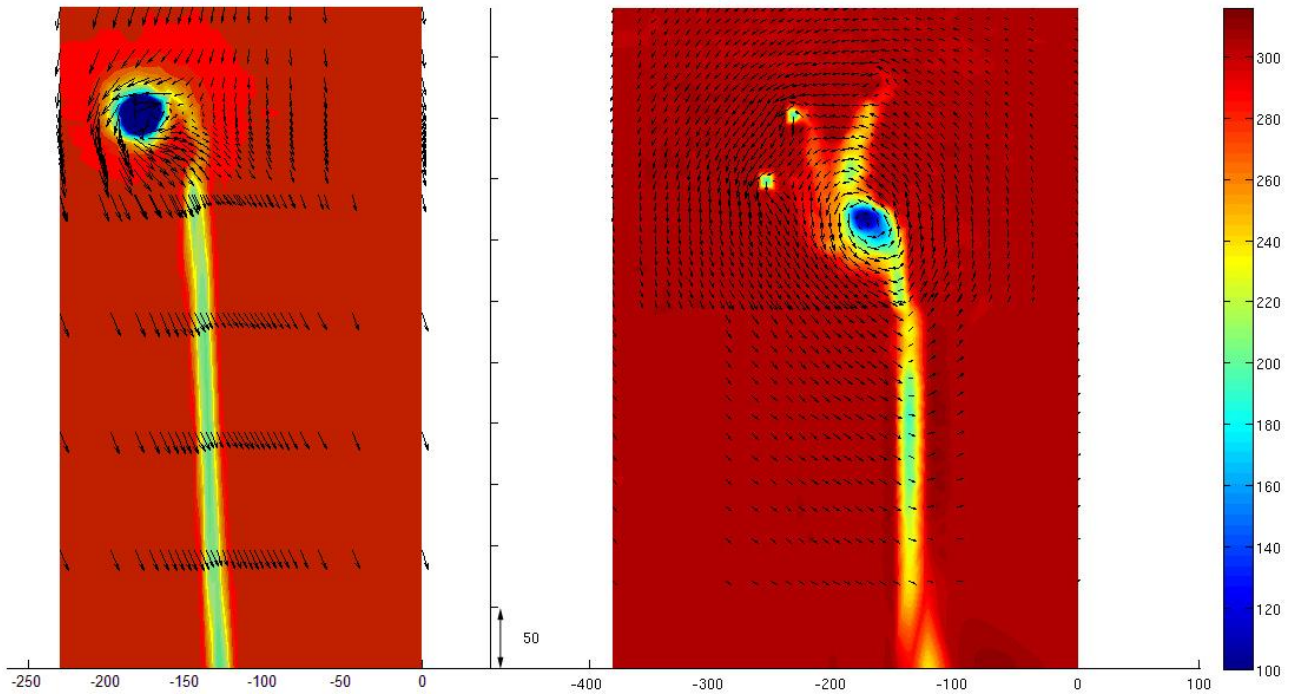


Figure 12. Dynamic pressure and velocity vector of the wake for baseline and first configuration

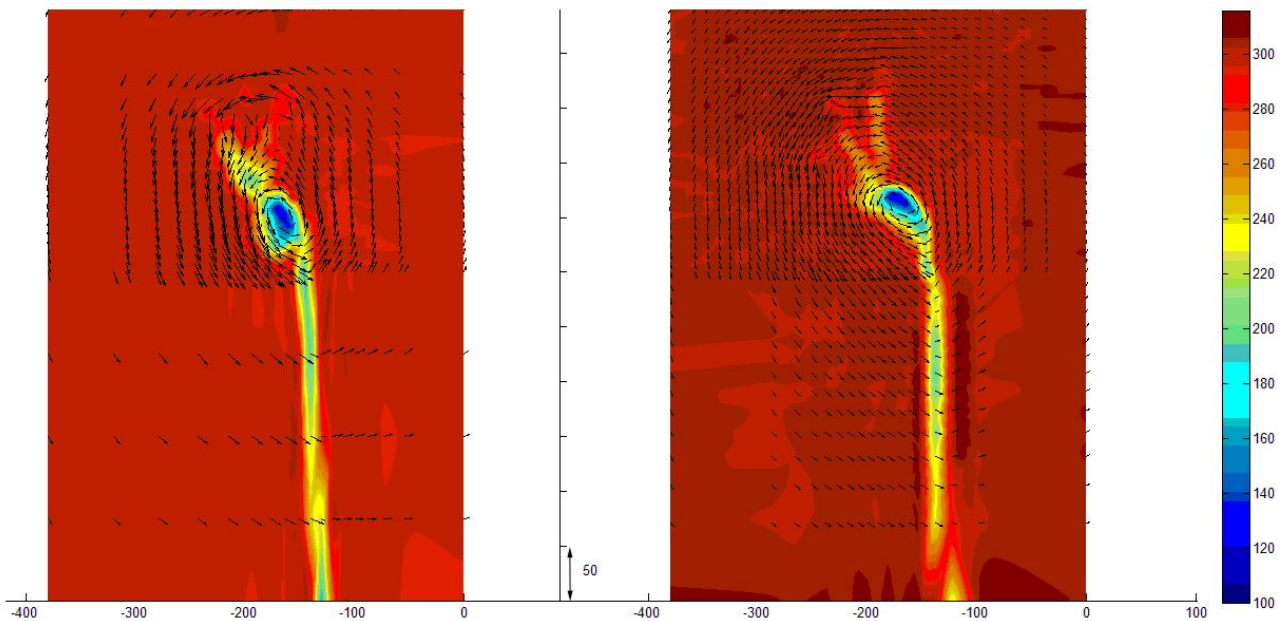


Figure 13. Dynamic pressure and velocity vector of the wake for third and sixth configuration

3.2.4. Flow visualization

“Figure 14” shows the steady flow visualization state for the multi-winglet sixth configuration for $\alpha = 4^\circ$. From this image is possibly to notice the interferences between the winglets tip vortex and the downstream sails, as well the interference of the wing tip over the sail in the region near their roots. It also stands out the laminar separation bubbles over the entire upper surface off all winglets.

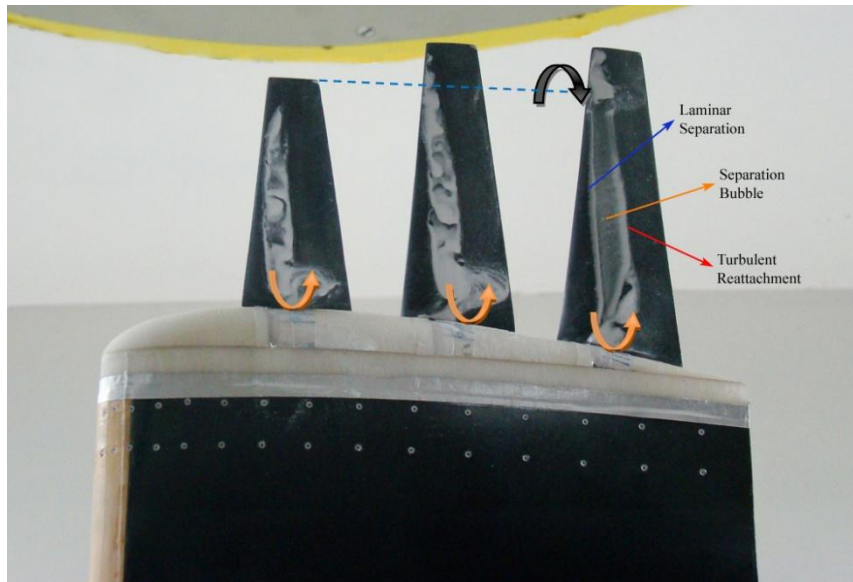


Figure 14. Flow visualization result illustration

3.3. Performance analysis

3.3.1. Aerodynamic efficiency

Enhancements on aerodynamic efficiency is a major objective of the use of multi-winglets. In “Fig 15” is possible to see the significant increases of lift-drag ratio due to the use of the tip device. These improvements are observed in most of useful angles of attack, specially for the higher ones. The increase on L/D reaches 11% for $\alpha = 8^\circ$ with the sixth configuration. The maximum efficiency was improved by up to 7.3% and for all the cases occurs on $\alpha = 4^\circ$.

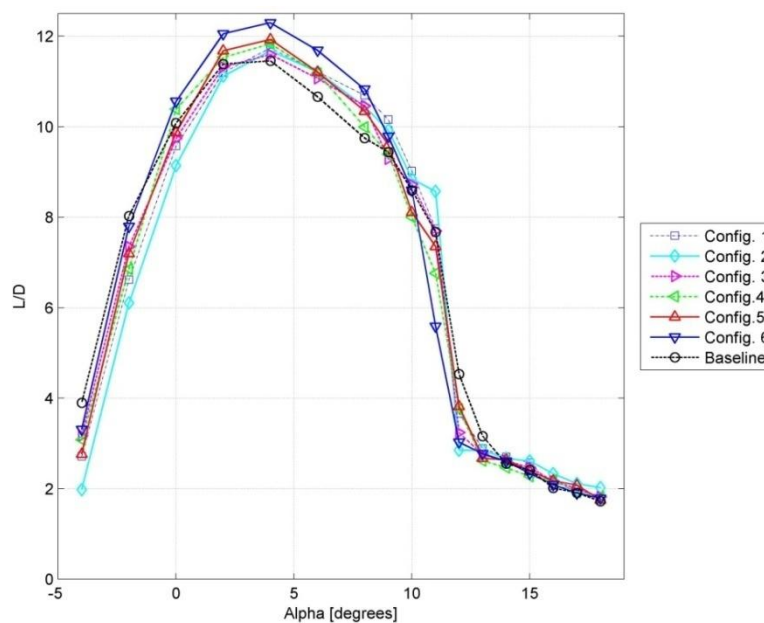


Figure 15. Aerodynamic efficiency curve

3.3.2. Rate o climb and range influence

Due to the gains in the lift and induced drag, the use of multi-winglets lead to expressive increases in the rate of climb, represented here by the rate of climb factor, $C_L^{1.5}/C_D$, as noticed on “Fig 16”. For the best condition, it was achieved 14% of improvement on this parameter. The maximum value increased 12%.

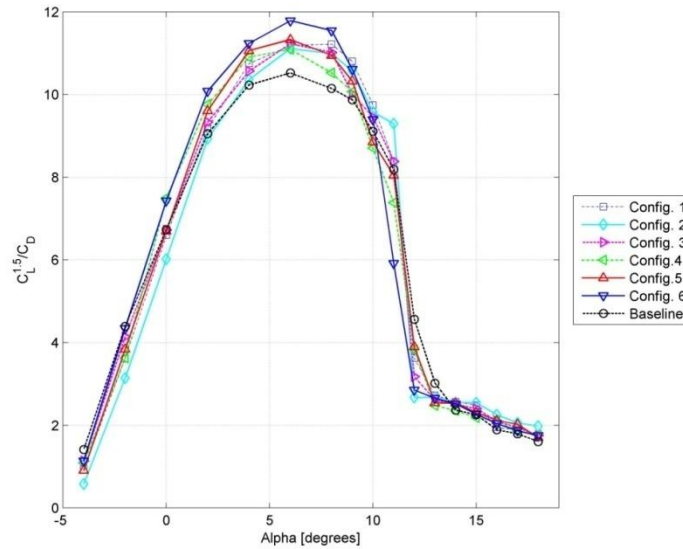


Figure 16. Climb rate factor curve

The effects on the range was analyzed by a range parameter, $C_L^{0.5}/C_D$, which revealed conditions of either improvements or losses. For lower angles of attack, the gains on induced drag didn't compensate the increase of C_{D_0} leading to worse values for the parameter. The maximum value of the parameter was decreased by 0.5% for the best configuration, however reached 8% of improvement for $\alpha = 8^\circ$.

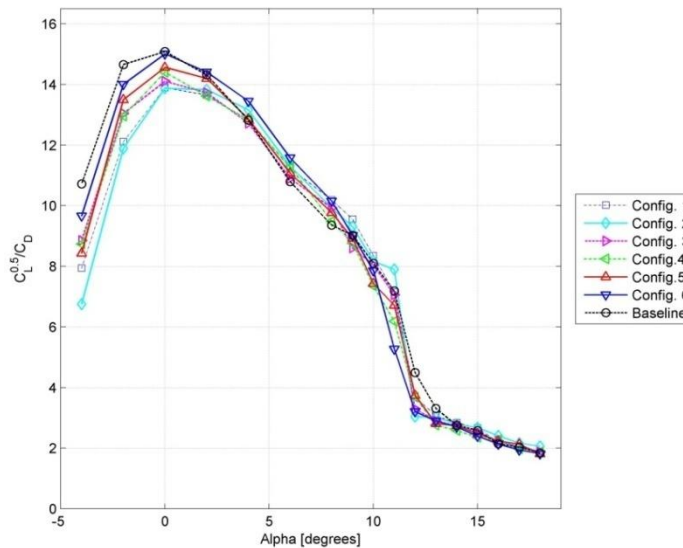


Figure 17. Range factor curve

3.4. Structural loading analysis

Direct measures of the bend moment were taken from the strain gage on the wing spar. These results revealed that the multi-winglets don't deteriorate the structural loading, maintaining the relation between the lift and the bend moment the same of those for the baseline configuration, as seen on “Fig 18”.

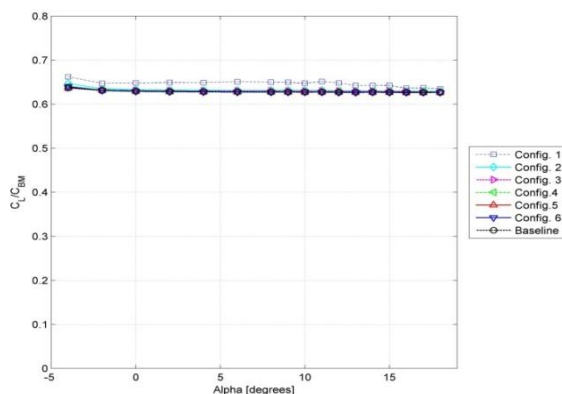


Figure 18. Lift to nondimensional bend moment ratio curve

4. CONCLUSIONS

The potential of improvements on aerodynamic efficiency by the use of multi-winglets was confirmed by the experimental data from this work. This wing tip device led to significant increases of the performance parameters, with a gain of 7.3% on maximum aerodynamic efficiency or 11% in best condition. The maximum rate of climb factor was also increased by 12%. The aerodynamic characteristics of the multi-winglets revealed improvements on lift values slope as well expressive results for the induced drag, represented by up to 32% of increase on the Oswald efficiency factor. However, the additional parasite drag due to the winglet withdraws the drag benefits for low lift conditions

The wing loading was slightly increased near the wingtip, maintaining, however, the general aspects of the baseline wing. These influences are a result of the weaker interference of the wing tip vortex over the wing, increasing lift and reducing induced drag. The wake analysis showed the significant decrease on the wing tip vortex intensity as well its break up thru the winglets. The structural loading relative to the lift was not changed by the use of the winglets bringing no negative effects to the structure.

5. ACKNOWLEDGMENTS

The authors would like to thank Fapesp for supporting this research project.

6. REFERENCES

- Cerón Muñoz, H. D and Catalano F. Experimental Analysis of the aerodynamic characteristics adaptive of multi-winglets. *Journal of Aerospace Engineering*, Vol. 220, No 3, pp. 209-216,
2006. Kravchenko S.A. The application of the wingtip lifting surfaces for practical aerodynamic. *ICAS-96-4.6.4*, pp 1338-1349, 1996.
- Whitcomb, R.T. A design approach and selected wind-tunnel results at high subsonic speeds for wing-tip mounted winglets. *NASA Technical note D-8260.*, pp 30, 1976.
- Spillman, The use of wing tip sails to reduce vortex drag. *J. J. Aeronautical Journal*, Vol. 82, No. 813, pp 387-395, 1978.
- Spillman, J. J. and McVitie, M. Wing tip sails which give lower drag at all normal flight speeds. *Aeronautical Journal*, Vol. 88, No. 878, pp 362-369, 1984.
- Spillman, J. J. Wing tip sails; progress to date and future developments. *Aeronautical Journal*, Vol 91 No 9XX, pp 445-543, 1987.
- Smith, M. J. Komerath, N. Ames, R. Wong, O. and Pearson, J. Performance analysis of a wing with multiple winglets. *AIAA paper 2001-2407*
- La Roche, U. And Palffy, S. Wing-grid, a novel device for reduction of induced drag on wings. *ICAS-96-2.10*, pp 2303-2309, 1996.
- Coimbra, R and Catalano, F. Estudo experimental sobre pontas de asa para uma aeronave agricola. *Revista Brasileira de Engenharia Agrícola e Ambiental*, Vol 3, No 1, pp 99-105, 1999
- Catalano, F. The new closed circuit wind tunnel of the aircraft laboratory of university of São Paulo. *16th Brazilian Congress of Mechanical Engineering*. Vol.6, pp 306-312, 2001

7. RESPONSIBILITY NOTICE

The authors are the only responsible for the material included in this paper.